

A statistical model prediction of effective electroelastic properties of polycrystalline ferroelectric ceramics with randomly oriented defects

Jinquan Cheng ^{*}, Biao Wang, Shanyi Du

Research Center for Composite Materials, Harbin Institute of Technology, P.O. Box 1247, Harbin 150001, PR China

Received 3 June 1999

Abstract

In terms of the microstructure characteristics of polycrystalline ferroelectric ceramics, a statistical micromechanics model is employed to predict the effective electroelastic properties of polycrystalline ferroelectric ceramics with randomly oriented defects, such as voids and microcracks, by the method of Eshelby's equivalent inclusion theory and Mori–Tanaka's mean field concept. The model incorporates the effects of crystallographic domain switching under external mechanical or electric field and the randomly oriented defects on the macroscopic behaviors of the polycrystalline ferroelectric ceramics. The analytical predictions of BaTiO₃ polycrystalline ceramics are shown that the defects can enhance the effective piezoelectric properties but reduce the elastic properties, which are consistent with the experimental results.

© 2002 Elsevier Science Ltd. All rights reserved.

Keywords: Polycrystalline ferroelectrics; Domain switching; Statistics; Micromechanics; Electroelastic properties

1. Introduction

Below Curie temperature, a ferroelectric crystal is composed of many regions, so-called domain, which exhibits a uniform spontaneous electrical polarization and strain field inside. For example, in tetragonal crystals, there are two types of do-

main wall that is the interface between the two adjacent domains existing: 180° and 90° domain wall. A suitable applied external electrical or mechanical field can cause a complicated course of 180° or 90° domain nucleation and domain wall motion, called domain switching. As a result of domain switching, the polarization and strain of individual grain change. An electrical field can re-orient both 180° and 90° domain, but a mechanical field only causes 90° domain switching. Only 90° domain switching has an effect on strain. Due to the particular microstructural 90° and 180° domain switching, ferroelectric ceramics exhibit the inherent ability to convert electrical to mechanical

^{*} Corresponding author. Present address: Institute of High Performance Computing, 1 Science Park Road, #01-01 The Capricorn, Singapore Science Park II, 117528 Singapore, Singapore. Tel.: +86-451-641-2613.

E-mail address: hitejq@hotmail.com (J. Cheng).

energy or mechanical to electrical energy (Jaff et al., 1971; Chueng and Kim, 1987; Zenon, 1994). Recently, ferroelectric ceramics play more important role in the applied functional ceramics since more and more smart structures, such as ultra-precise displacement transducers and actuators, are mostly made of ferroelectric ceramics. Ferroelectric ceramics have such a wide variety of applications that many researchers are interested in investigating their production process and properties. Generally, ferroelectric ceramics are prepared by sintering compressed powers of oxide, leading to a polycrystalline microstructure, which is a unpoled macroscopically isotropic ferroelectric ceramic with a variety of defects, such as voids (Chueng and Kim, 1987), after cooling below Curie temperature. For unpoled ferroelectric ceramics, the effective polarization of ferroelectric crystallite, which is the vector sum of the polarization of each domain in individual crystal, is randomly arranged so as to show macroscopically isotropic and non-piezoelectric. But after a sufficient external electric field applied, the complicated domain switching results in reorienting the effective polarization of each crystal to be approximated to the applied electric field direction in this way to minimize the body energy. After the process of “poling” or “polarizing”, the ferroelectric ceramics can exhibit piezoelectric property and be suitable for as functional materials. Domain switching is not only well-known to result in a non-linear hysteretic phenomena (Cao and Evans, 1993; Ansgar et al., 1996) but also create large internal stress field, leading to intergranular microcracking, which can degrade (or possibly enhance) the macroscopic properties of the overall ceramics (Kahn, 1985; Lynch et al., 1995; Zhang et al., 1997). So a typical poled ferroelectric ceramics usually contains a few of defects such as voids and microcracks. Then their overall behaviors are directly related to the microstructure characteristics of the materials, which are difficult to be predicted. In theory, Deeg (1980), Wang (1992a,b) and Benveniste (1992) independently extended Eshelby’s classical work to a piezoelectric ellipsoidal inclusion embedded in a piezoelectric matrix. Marutak (1965), Benveniste and Dvorak (1992), Dunn and Taya (1993a) and Wang (1994)

studied the effective properties of ideal fully bonded piezoelectric ceramics without considering the effect of the microstructural evolution inherent in ferroelectric ceramics. In addition, Nan and Clarke (1996) and Kuo and Huang (1997) analyzed the effective modulus of fully bonded piezoelectric ceramic, considering the effects of shape and orientations of individual grains. Dunn and coworkers (1993b, 1993c, 1995) adopted the micromechanical method to predict effective modulus of unpoled polycrystalline piezoelectric ceramic with defects. They did not take the relative microstructure evolution of ferroelectric ceramics into account. Recently in order to consider the effects of the microstructure evolution of ferroelectric ceramics, Chen et al. (1997a,b) had established a mesoscopic model and then used the micromechanics method to study the constitutive behavior of monocrystalline and polycrystalline ferroelectrics. Hwang et al. (1995) established a one-dimensional model to analyze the relation between domain switching and electroelastic properties for ferroelectric/ferroelastic ceramics. In this paper, based on the microstructure-level evolution characteristics inherent in the ferroelectric ceramics, we develop the Eshelby’s model with Mori–Tanaka’s mean field theory and statistical model to predict the effective electroelastic properties of polycrystalline ferroelectric ceramics with randomly oriented defects such as microcracks and voids. The proposed model accounts for the influences of randomly oriented defects and domain switching on the effective electroelastic properties under the application of the external field.

2. Fundamental formulations and notations

In absence of body forces or free charge, the static elastic and electric field equations can be given by the equations of elastic equilibrium and Gauss’s law of electrostatics among the strain ε_{ij} , stress σ_{ij} , electric field E_i , elastic displacement u_i , electric potential ϕ and electric displacement D_i as follows:

Divergence equations:

$$\begin{aligned}\sigma_{ij,j} &= 0 \\ D_{i,j} &= 0\end{aligned}\tag{1}$$

Gradient equations:

$$\begin{aligned}\varepsilon_{ij} &= \frac{1}{2}(u_{i,j} + u_{j,i}) \\ E_i &= -\phi_{,i}\end{aligned}\quad (2)$$

Constitutive equations:

$$\begin{aligned}\sigma_{ij} &= C_{ijmn}\varepsilon_{mn} + e_{nij}\phi_{,n} \\ D_i &= e_{imn}\varepsilon_{mn} - k_{in}\phi_{,n}\end{aligned}\quad (3)$$

where C_{ijmn} is the elastic modulus (measured in constant electric field), e_{nij} is the piezoelectric modulus (measured at a constant strain or electric field), and k_{in} is the dielectric modulus (measured at a constant strain), respectively.

Based on the notation introduced by Barnett and Lothe (1975), we can conveniently represent the above equations in a simply form as

$$Z_{Mn} = \begin{cases} \varepsilon_{mn} & M = 1, 2, 3 \\ \phi_{,n} & M = 4 \end{cases}\quad (4)$$

where Z_{Mn} is derived from U_M given by

$$U_M = \begin{cases} u_m & M = 1, 2, 3 \\ \phi & M = 4 \end{cases}\quad (5)$$

Similarity the stress and electric displacement are represented as

$$\Sigma_{iJ} = \begin{cases} \sigma_{ij} & J = 1, 2, 3 \\ D_i & J = 4 \end{cases}\quad (6)$$

The electroelastic modulus can then be represented as

$$E_{iJMn} = \begin{cases} C_{ijmn} & J, M = 1, 2, 3 \\ e_{nij} & J = 1, 2, 3; M = 4 \\ e_{imn} & J = 4; M = 1, 2, 3 \\ -k_{in} & J, M = 4 \end{cases}\quad (7)$$

Noted that the “inverse” of E_{iJMn} is defined as F_{AbiJ} , evidently both E_{iJMn} and F_{AbiJ} are diagonally symmetric for transversely isotropic piezoelectric ceramics.

In order to be convenient to derive the equations, we can represent Eqs. (4)–(7) as 9×1 and 9×9 matrices by utilizing the mapping of adjacent indices, e.g. $(iJ) = (Ji)$ and $(Mn) = (nM)$ for J and $M \neq 4$:

$$\begin{aligned}(11) &\rightarrow 1, (22) \rightarrow 2, (33) \rightarrow 3, (23) \rightarrow 4, \\ (13) &\rightarrow 5, (12) \rightarrow 6, (14) \rightarrow 7, (24) \rightarrow 8, \\ (34) &\rightarrow 9\end{aligned}$$

Based upon the mapping, we can simplify those mentioned expressions as matrixes in order to induce conveniently in the next section. So the constitutive relations can be represented as matrixes:

$$\Sigma_{9 \times 1} = E_{9 \times 9} Z_{9 \times 1}$$

$$Z_{9 \times 1} = F_{9 \times 9} \Sigma_{9 \times 1}$$

3. The Eshelby–Mori–Tanaka theory for polycrystalline ferroelectric ceramics with randomly arranged defects

3.1. A statistical micromechanics model

Since the ferroelectric ceramics have the particular microstructure domain, and individual crystal consists of many domains below Curie temperature, we can regard the effective polarization of individual crystal as the vector sum of each domain inside it. At room temperature, for unpoled ferroelectric ceramics with randomly oriented voids, the effective polarization of individual grain randomly distributes, shown in Fig. 1(a). When the ferroelectric ceramics subjected to a strong electric field, all the domains switch (two mechanism: nucleation and domain-wall motion) so that the effective polarization of individual grain would be approximated to the applied electrical field direction in order to minimize the body energy. In a consequence of domain switching, large internal stress is generated around the grain boundary and results in microcracking, shown in Fig. 1(b). On the basis of the experimental observations of domain switching current, Merz (1956) concluded that the domain switching is mostly a nucleation problem. So, it is efficient to use the Kolmogorov–Avrami (K–A) statistical theory to describe the process of domain switching. Thus, the probability of domain switching (nucleation) along the direction of applied electric field can be obtained by the experimental results (Merz, 1956; Xu, 1991):

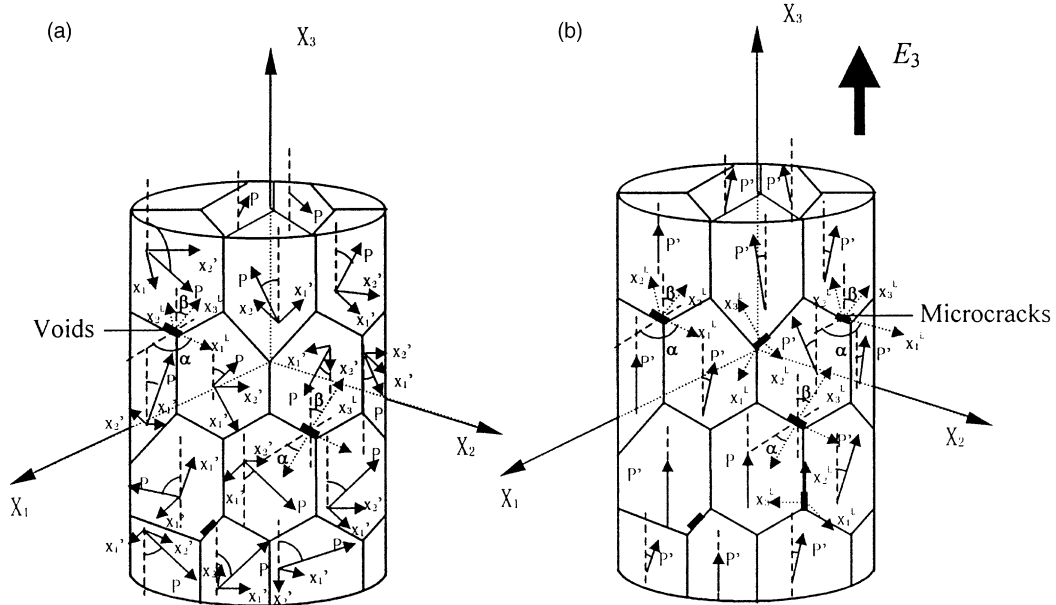


Fig. 1. The model showing the unpoled (a), poled (b) ceramics and individual domain switching under the action of external field.

$$P = P_0 \exp\left(-\frac{b}{E}\right) \quad (8)$$

where, b is the threshold value of activate electric field. For a BaTiO_3 ceramic, the threshold field b along the poling direction is 470 kV/m. P_0 is the probability of domain switching under the action of infinite external electric field E_i ($i = x, y$ or z). The probability of domain switching determined by Eq. (8) only depends on the applied electric field. Under the action of the external mechanical field, we can roughly “transfer” the applied mechanical field into the relative electric field through the piezoelectric constitutive equations in order to use Eq. (8).

By means of Eshelby’s equivalent inclusion principle, we regard the newly switched grain due to the external electric or mechanical field and the spatially distributed defect as composed of two phase inclusions ($r = 1, 2$) and the initially poled ceramics (matrix). Then, the mean field of the matrix with electroelastic modulus E_m may differ from Σ^0 by a disturbed field Σ^1 , given by

$$\Sigma_m = \Sigma^0 + \Sigma^1 = E_m(Z^0 + Z^1) \quad (9)$$

where Σ^1, Z^1 are the average disturbance fields due to the presence of piezoelectric inhomogeneities and the interactions among the inclusions.

For the first phase inclusion, the newly switched crystals, with electroelastic constant E_1 , occupy a region Ω_1 . Due to their local coordinate system consistent with the fixed or material coordinate system as a consequence of domain switching, we can represent the electroelastic field in the newly switched crystal as

$$\begin{aligned} \Sigma_1 &= \Sigma^0 + \Sigma^1 + \Sigma_1^{\text{pt}} \\ &= E_1(Z^0 + Z^1 + Z_1^{\text{pt}} - Z_1^*) \\ &= E_m(Z^0 + Z^1 + Z_1^{\text{pt}} - Z_1^* - Z_1^{**}) \end{aligned} \quad (10)$$

where Z_1^{pt} represents the perturbation of the strain and electric fields in the newly switched crystal with respect to those in the matrix. Z_1^* is the spontaneous eigenfield: strain and electric field and Z_1^{**} is the fictitious eigenfield due to the inhomogeneity.

For the second phase inclusion, defects, are spatially distributed in the matrix and occupy the region Ω_2 , we can also express the electrical and mechanical field in the defect by the way of

Eshelby's equivalent inclusion theory in the local coordinate system:

$$\begin{aligned}\Sigma_2^L &= \Sigma^{0L} + \Sigma^{1L} + \Sigma_2^{\text{pt}L} = 0 \\ &= E_m(Z^{0L} + Z^{1L} + Z_2^{\text{pt}L} - Z_2^{*L})\end{aligned}\quad (11)$$

where the superscript 'L' denotes the local coordinate system. For the randomly arranged defects, we can assume that the fixed coordinate system is denoted as (x_1, x_2, x_3) . The local coordinate system can be established by (x_1^L, x_2^L, x_3^L) , x_3^L is the symmetric axis like fixed coordinate and let x_1^L lies in (x_1, x_2) plane with no loss in generality, as shown in Fig. 1. Then, we can obtain the transformed matrix T from fixed to local coordinate system:

$$T_{ij} = \begin{bmatrix} \cos \alpha & \sin \alpha & 0 \\ -\sin \alpha \cos \beta & \cos \alpha \cos \beta & \sin \beta \\ \sin \alpha \sin \beta & -\sin \beta \cos \alpha & \cos \beta \end{bmatrix}$$

then

$$\begin{aligned}\varepsilon_{ij}^L &= T_{im} T_{jn} \varepsilon_{mn} \\ E_i^L &= T_{in} E_n\end{aligned}\quad (12)$$

Reducing Eq. (12) can lead to the matrix form:

$$Z^L = [A]Z \quad (13)$$

where $[A]$ is the transformed matrix from fixed to local coordinate system.

In accordance with the electroelastic Eshelby's tensor S derived from Wang (1992a)'s three-dimensional solution of an ellipsoidal inclusion in a piezoelectric material (see Appendix A), Z_r^{pt} , the disturbed field about two phase ($r = 1, 2$), can be obtained:

$$\begin{aligned}Z_1^{\text{pt}} &= S_1(Z_1^* + Z_1^{**}) \\ Z_2^{\text{pt}L} &= S_2 Z_2^{*L}\end{aligned}\quad (14)$$

Further by the transformed matrix,

$$Z_2^{\text{pt}} = [A]^{-1} S_2 [A] Z_2^* \quad (15)$$

Substitution of Eq. (14) into Eqs. (10) and (11) yields:

$$\begin{aligned}Z_1^{**} &= [E_1 S_1 - E_m (S_1 - I)]^{-1} (E_m - E_1) \\ &\quad \times [Z^0 + Z^1 + (S_1 - I) Z_1^*]\end{aligned}\quad (16a)$$

$$Z_2^{*L} = -(S_2 - I)^{-1} (Z^{0L} + Z^{1L}) \quad (16b)$$

On the basis of the transformed principle, we can lead to

$$Z_2^* = -[A]^{-1} (S_2 - I)^{-1} [A] (Z^0 + Z^1) \quad (17)$$

3.2. Traction–electric displacement prescribed boundary condition

When subjected to a far-field traction and electric displacement, $\Sigma_{ij}^0 n_i$, on the boundary with outward unit normal vector n_i , the average field of overall ceramic can be obtained by the Mori–Tanaka's mean field approach:

$$\begin{aligned}\langle \Sigma \rangle &= \frac{1}{V} \int_{D-\Omega_1-\Omega_2} \Sigma_m dv + \frac{1}{V} \int_{\Omega_1} \Sigma_1 dv + \frac{1}{V} \int_{\Omega_2} \Sigma_2 dv \\ &= \Sigma^0 = \frac{1}{V} \int_{D-\Omega_1-\Omega_2} E_m (Z^0 + Z^1) dv \\ &\quad + \frac{1}{V} \int_{\Omega_1} E_m (Z^0 + Z^1 + Z_1^{\text{pt}} - Z_1^* - Z_1^{**}) dv \\ &\quad + \frac{1}{V} \int_{\Omega_2} E_m (Z^0 + Z^1 + Z_2^{\text{pt}} - Z_2^*) dv\end{aligned}\quad (18)$$

then,

$$\begin{aligned}0 &= \frac{1}{V} \int_{D-\Omega_1-\Omega_2} E_m Z^1 dv \\ &\quad + \frac{1}{V} \int_{\Omega_1} E_m (Z^1 + Z_1^{\text{pt}} - Z_1^* - Z_1^{**}) dv \\ &\quad + \frac{1}{V} \int_{\Omega_2} E_m (Z^1 + Z_2^{\text{pt}} - Z_2^*) dv\end{aligned}\quad (19)$$

Since the defects are three-dimensional randomly distributed in the matrix, the distribute functions of the defects can be obtained by $f = (1/2\pi) \sin \beta$, then Z^1 can be deduced to

$$Z^1 = -v_1 (S_1 - I) (Z_1^* + Z_1^{**}) - v_2 \langle Z_2^{\text{pt}} - Z_2^* \rangle \quad (20)$$

where

$$\begin{aligned}\langle Z_2^{\text{pt}} - Z_2^* \rangle &= \frac{1}{2\pi} \int_0^\pi \int_0^\pi \sin \beta [A]^{-1} (S_2 - I) \\ &\quad \times [A] Z_2^* d\beta d\alpha\end{aligned}\quad (21a)$$

$$\langle Z_2^* \rangle = \frac{1}{2\pi} \int_0^\pi \int_0^\pi \sin \beta Z_2^* d\beta d\alpha \quad (21b)$$

Combining Eq. (17), (20) and (21a) and (21b) leads to

$$Z^1 = \frac{1}{(1-v_2)} [Z^0 - v_1(S_1 - I)(Z_1^* + (Z_1^{**}))] \quad (22)$$

Substituting Eq. (22) into Eq. (16a) can yield

$$\begin{aligned} Z_1^{**} = & \left[E_1 S_1 - E_m(S_1 - I) + \frac{v_1}{1-v_2} \right. \\ & \times (E_m - E_1)(S_1 - I) \left. \right]^{-1} (E_m - E_1) \\ & \times \left[\frac{1}{1-v_2} Z^0 + \frac{1-v_1-v_2}{1-v_2} (S_1 - I) Z_1^* \right] \quad (23) \end{aligned}$$

Based on Eq. (17), (22) and (23), it is easy to derive the expression of Z_2^* .

On the other hand, the overall strain and electric field denoted by $\langle Z \rangle$ can be obtained as the weighted average of over each phase:

$$\begin{aligned} \langle Z \rangle = & \frac{1}{V} \left[\int_{D-\Omega_1-\Omega_2} (Z^0 + Z^1) dv \right. \\ & + \int_{\Omega_1} (Z^0 + Z^1 + Z_1^{\text{pt}} - Z_1^*) dv \\ & \left. + \int_{\Omega_2} (Z^0 + Z^1 + Z_2^{\text{pt}}) dv \right] \\ = & Z^0 + v_1 Z^{**} + v_2 \langle Z_2^* \rangle \quad (24) \end{aligned}$$

If it is assumed that there are total N potential switching grains in volume V , the average number n of the newly switched grain for a given electrical or mechanical field:

$$n = N \cdot P \quad (25)$$

where P is defined in Eq. (8).

So the volume fraction v_1 of the newly switched grain along the direction of the applied or equivalent electric field can be obtained by

$$v_1 = n \cdot v / V = N \cdot P \cdot v / V = v_1^0 \cdot P \quad (26)$$

where v_1^0 is the volume fraction of all the potential switchable crystals and v is the volume of individual crystal.

Now combining Eqs. (21a)–(24) and (26), we can obtain the expression for the effective electro-elastic behavior and effective constant E^* , consid-

ering the particular microstructure-level evolution of ferroelectric ceramics as following:

$$\langle \Sigma \rangle = E^* \langle Z \rangle = \Sigma^0 \quad (27)$$

3.3. Elastic displacement–electric field prescribed boundary condition

Let the ferroelectric ceramics be subjected to a far-field applied elastic displacement and electric field Z_{mn}^0 , in terms of the Mori–Tanaka's mean field concept, the overall average electric field and strain field can be obtained as

$$\begin{aligned} Z^0 = & \frac{1}{V} \int_{D-\Omega_1-\Omega_2} (Z^0 + Z^1) dv \\ & + \frac{1}{V} \int_{\Omega_1} (Z^0 + Z^1 + Z_1^{\text{pt}} - Z_1^*) dv \\ & + \frac{1}{V} \int_{\Omega_2} (Z^0 + Z^1 + Z_2^{\text{pt}}) dv \end{aligned}$$

Based on Eqs. (14), (15) and (17), we can obtain:

$$Z^1 = (I - v_2 B)^{-1} [v_2 B Z^0 - v_1(S_1 - I)Z_1^* - v_1 S_1 Z_1^{**}] \quad (28)$$

where

$$B = -\frac{1}{2\pi} \int_0^\pi \int_0^\pi \sin \beta [A]^{-1} S_2 (S_2 - I)^{-1} [A] d\beta d\alpha$$

Combining Eqs. (16a) and (28) leads to

$$\begin{aligned} Z_1^{**} = & [E_1 S_1 - E_m(S_1 - I) + v_1(E_m - E_1) \\ & \times (I - v_2 B)^{-1} S_1]^{-1} (E_m - E_1) \\ & \times \{ [I + v_2(I - v_2 B)^{-1} B] Z^0 \\ & + [I - v_1(I - v_2 B)^{-1}] (S_1 - I) Z_1^* \} \quad (29) \end{aligned}$$

The overall stress and electric displacement of ceramic, $\langle \Sigma_{ij} \rangle$, can be obtained in a manner as the definition of Eq. (24) as

$$\begin{aligned} \langle \Sigma \rangle = & \frac{1}{V} \int_{D-\Omega_1-\Omega_2} \Sigma_m dv + \frac{1}{V} \int_{\Omega_1} \Sigma_1 dv \\ & + \frac{1}{V} \int_{\Omega_2} \Sigma_2 dv \end{aligned}$$

Then, the effective properties of stress and electric displacement of overall ceramics can be shown as

$$\langle \Sigma \rangle = E_m \langle Z^0 - v_1 Z_1^{*} - v_2 \langle Z_2^* \rangle \rangle \quad (30)$$

Thus, we can present the effective electroelastic properties of polycrystalline ferroelectric ceramics as

$$\langle Z \rangle = F^* \langle \Sigma \rangle = Z^0 \quad (31)$$

It is well known that the poled ferroelectric ceramic is transversely isotropic with the x_3 -axis being the poling axis. Generally, the crystal of commercially valuable ferroelectric ceramics belongs to the class 6 mm or 4 mm symmetry, which exhibits transversely isotropic properties. Since Dunn and Taya (1993c) has shown that the shape of domains (inclusions) has relatively little influence on the macroscopic behavior of the ferroelectric ceramics, it is reasonable to assume the shape of the crystal as spheroidal for mathematical convenience in theory. As he previously mentioned, the newly switched crystals are arranged in such way their symmetric axes are in parallel with the x_3 -axis. Therefore, in the case of only considering randomly oriented defects, it is easy to show that the effective ceramics are also transversely isotropic with the x_3 -axis to be the symmetric axis. Thus, the effective electroelastic modulus E^* and F^* predicted by the proposed model are also diagonal symmetry.

4. Numerical examples and discussion

In this section, we will use the presented model to predict the effective properties of BaTiO₃ ceramics, which were discovered and applied in the engineering field as functional materials early. Jaff et al. (1971) had measured the elastic, dielectric and piezoelectric coefficients of single-crystal and polycrystalline ceramics of BaTiO₃, shown in Table 1. At the room temperature, the tetragonal phase of BaTiO₃ with the cell parameters $a = 3.992 \text{ \AA}$ and $c = 4.032 \text{ \AA}$ has the spontaneous polarization $P_s = 0.26 \text{ C/m}^2$ and the remanent

Table 1

The elastic, piezoelectric and dielectric coefficients of BaTiO₃ at 25° (Jaff et al., 1971)

	Single-crystal	Ceramic
C_{11}^E (GPa)	275	166
C_{33}^E (GPa)	164.8	162
C_{44}^E (GPa)	54.3	43
C_{12}^E (GPa)	178.9	77
C_{13}^E (GPa)	151.6	78
e_{31} (C/m ²)	−2.69	−4.4
e_{33} (C/m ²)	3.65	18.6
e_{15} (C/m ²)	21.3	11.6
$k_{11} \times 10^{-9} \text{ C}^2 \text{ N}^{-1} \text{ m}^{-2}$	17.4	11.2
$k_{33} \times 10^{-9} \text{ C}^2 \text{ N}^{-1} \text{ m}^{-2}$	0.96	12.6
$d_{31} \times 10^{-12} \text{ C/N}$	−34.5	−79
$d_{33} \times 10^{-12} \text{ C/N}$	85.6	191
$d_{15} \times 10^{-12} \text{ C/N}$	392	270

polarization $P_r = 0.08 \text{ C/m}^2$. Therefore, the eigen-strain and eigenelectric displacement of a single-crystal can be given:

$$\varepsilon^* = \begin{bmatrix} -0.005 & 0 & 0 \\ 0 & -0.005 & 0 \\ 0 & 0 & 0.01 \end{bmatrix}$$

$$D^* = [0 \quad 0 \quad 0.26]^T$$

In terms of the material electroelastic coefficients shown in Table 1 and the threshold field b is 470 kV/m, the effective properties of polycrystalline BaTiO₃ ceramics with three-dimensional distributed penny-shape defects are predicted by using Eqs. (27) and (31) on the assumption of spherical crystal. In order to utilize the experimental results of BaTiO₃ and simplify the calculation process, we only consider two cases of the applied external fields: (1) an applied electric field E_3 along the poling direction, (2) the compressive stress $\sigma_{11} = \sigma_{22}$ which can be transferred to the equivalent electric field along the poling direction by the constitutive relationship. Fig. 2 shows the effective piezoelectric modulus d_{33} as a function of the applied external field E_3 and the volume fraction v_2 of defects. From Fig. 2, it is evident that the value of d_{33} increases with increasing the volume fraction v_2 of defects in any case. Fig. 2 also presents that the

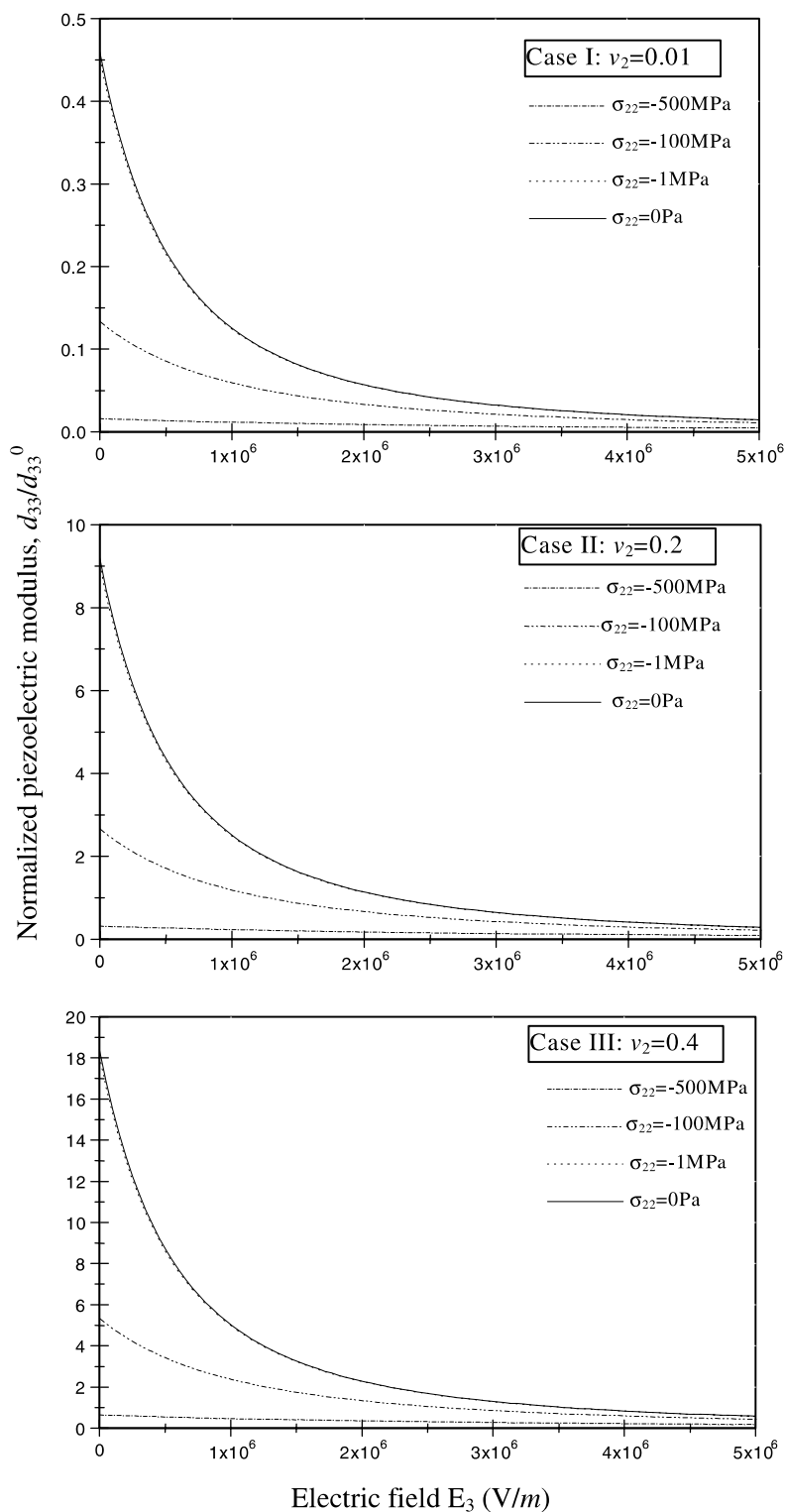


Fig. 2. The effects of the external applied electrical, mechanical field and the volume fraction v_2 of defects on effective piezoelectric modulus d_{33} of BaTiO₃ ceramics.

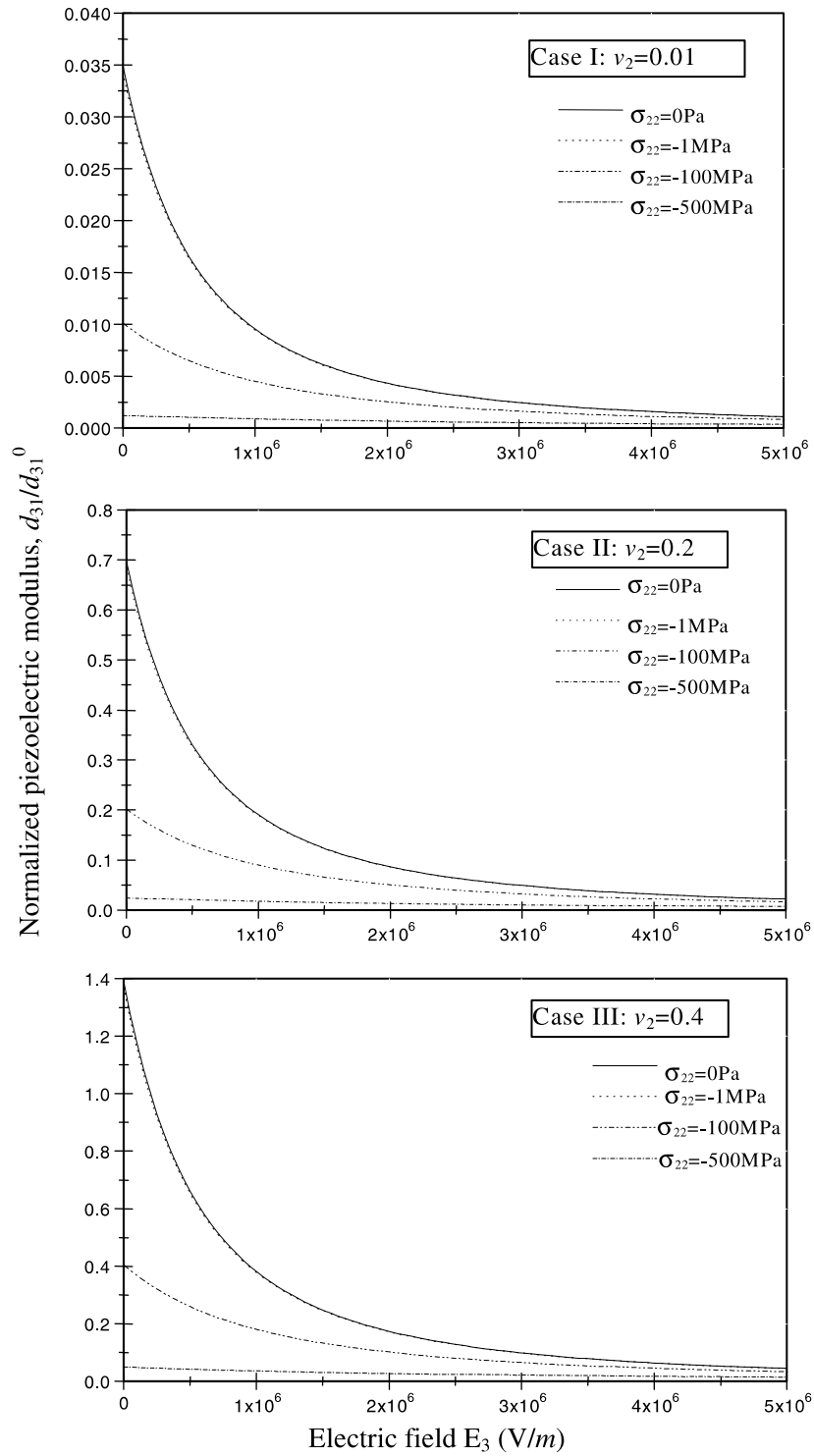


Fig. 3. Influences of the external applied electrical, mechanical field and volume fraction v_2 of defects on effective piezoelectric modulus d_{31} of BaTiO₃ ceramics.

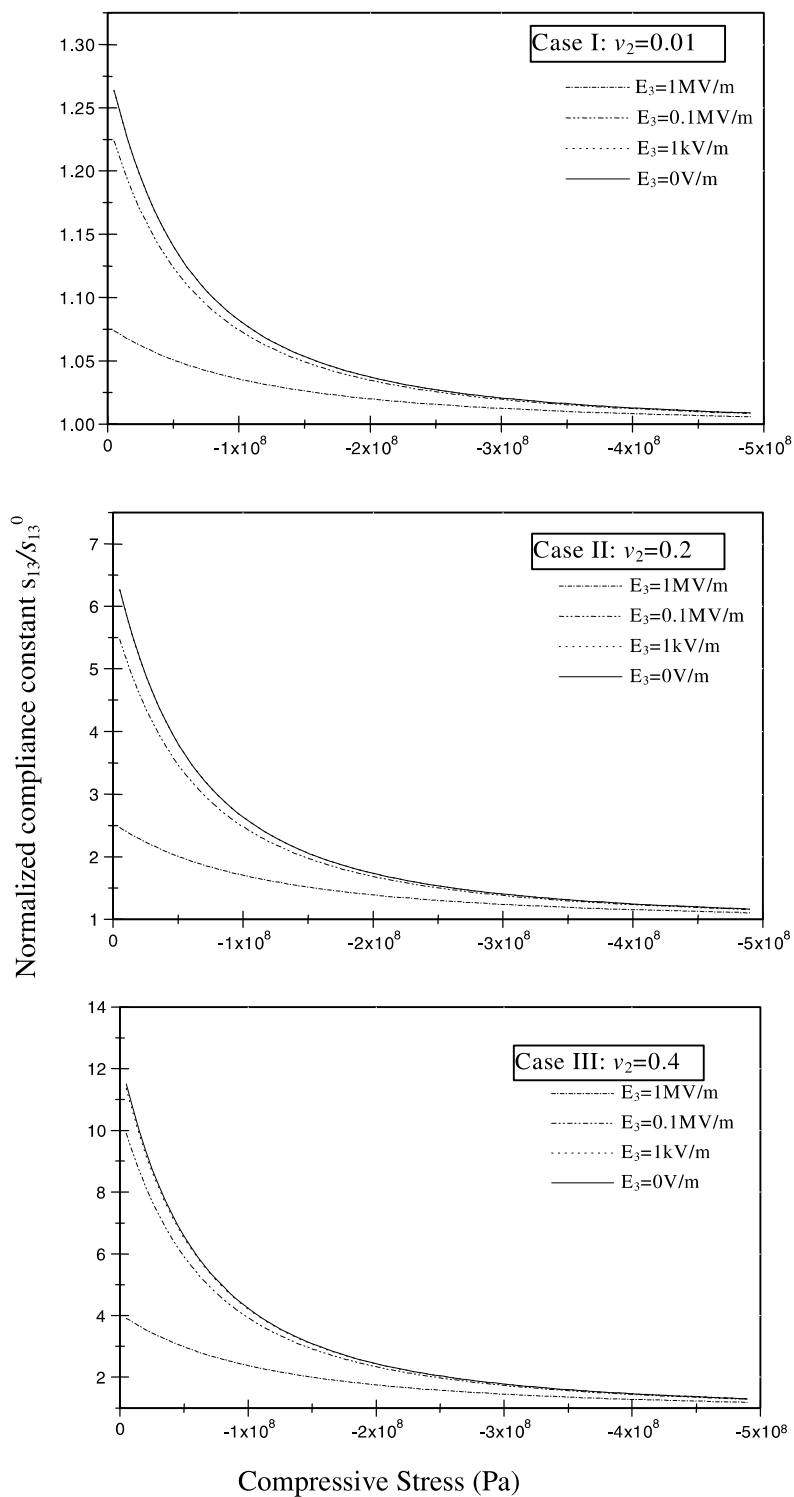


Fig. 4. The effects of the external applied electrical and mechanical field, volume fraction v_2 of defects on effective compliance constant S_{13} of BaTiO₃ ceramics.

effective piezoelectric modulus d_{33} decreases non-linearly when the external applied electric or compressive stress field increases. Moreover, as the applied stress reaches a sufficiently strong value, d_{33} would become zero in a sense. These results can be interpreted as the effects of microstructure evolution under the application of external field: an electric field can cause both 180° and 90° domain switching; But mechanical field can only reorient 90° domain. Thus, all the 90° domains would be reoriented under the action of the enough large mechanical field. Even a strong applied electric field only causes 180° domain reoriented, which do not result in the strain change. According to the definition of d_{33} : $d_{33} = \partial \epsilon_{33} / \partial E_3$, d_{33} would approach to zero by the definition theoretically. Simultaneously, while a sufficiently strong electric field reorients all the potential switchable domains, the ceramics would exhibit linear elasticity properties as well as the experimental observation (Cao and Evans, 1993). Fig. 3 gives the effective piezoelectric modulus of d_{31} as a function of external field and the volume fraction v_2 of defects. It is seen that the presence of defects can improve the piezoelectric modulus d_{31} in a sense. And, d_{31} increases non-linearly as the applied external electrical or mechanical field increases. Additionally, Fig. 4 shows the compliance constant changes with the applied external field E_3 and the volume fraction v_2 of defects. The compliance constant S_{13} decreases non-linearly by the volume fraction v_2 of defects increasing in any case. But while the applied electric field reaches a sufficiently high value, the effect of the volume fraction v_2 of defects on the compliance constant is similar to that of linear elastic material. Since a sufficiently strong electrical field has caused all the 180° and 90° domains switching, the ceramics would not exhibit piezoelectric properties but like the normal linear elastic material. These predictions confirm the fact that the overall macroscopic behavior of ferroelectric ceramics are associated with the microstructure-level evolution and agree well with the experimental results: The elastic properties of the polycrystalline ferroelectric ceramics decrease but enhance the piezoelectric properties due to the presence of defects (Kahn, 1985; Dunn and Taya (1993a,b,c); Dunn, 1995).

5. Conclusion

In accordance with polycrystalline ferroelectric ceramics microstructural evolution phenomena and classical nucleation theory, we establish a micromechanic model to investigate the effects of external field inducing domain switching and randomly distributed defects on the effective electroelastic properties of polycrystalline ferroelectric ceramics. In the procedure of solution, we adopt Wang (1992a)'s three-dimensional solutions for an ellipsoidal piezoelectric inclusion in piezoelectric materials and Eshelby–Mori–Tanaka's method. For example, the effective electroelastic behavior and constants of BaTiO_3 ceramics with randomly oriented defects are numerically analyzed. These results confirm that the defect can enhance the piezoelectric properties but decrease the elastic properties of ferroelectric ceramics. The predictions are in agreement with the experimental results.

Acknowledgements

This work was supported by the National Foundation of China for Excellent Young Investigators.

Appendix A

The electroelastic Eshelby tensors S can be obtained on the basis of Wang (1992a)'s three-dimensional solution of a spheroidal inclusion in a piezoelectric material in the following form:

$$S = \begin{bmatrix} S_{11} & S_{12} & S_{13} & S_{14} & S_{15} & 0 & 0 & 0 & S_{19} \\ S_{21} & S_{22} & S_{23} & S_{24} & S_{25} & 0 & 0 & 0 & S_{29} \\ S_{31} & S_{32} & S_{33} & S_{34} & S_{35} & 0 & 0 & 0 & S_{39} \\ S_{41} & S_{42} & S_{43} & S_{44} & S_{45} & 0 & 0 & S_{48} & 0 \\ S_{51} & S_{52} & S_{53} & S_{54} & S_{55} & 0 & S_{57} & 0 & 0 \\ 0 & 0 & 0 & 0 & 0 & S_{66} & 0 & 0 & 0 \\ 0 & 0 & 0 & 0 & S_{75} & 0 & S_{77} & 0 & 0 \\ 0 & 0 & 0 & S_{84} & 0 & 0 & 0 & S_{88} & 0 \\ S_{91} & S_{92} & S_{93} & 0 & 0 & 0 & 0 & 0 & S_{99} \end{bmatrix}$$

The non-zero components of matrix $[S]$ are presented as following:

$$\begin{aligned}
S_{11} &= \frac{1}{4\pi} (C_{11}^0 N_{1111}^1 + C_{12}^1 N_{1212}^1 + C_{31}^0 N_{1313}^1 + e_{31}^0 N_{113}^2) & S_{39} &= -\frac{1}{4\pi} (e_{31}^0 N_{1313}^1 + e_{32}^0 N_{1323}^1 + e_{33}^0 N_{1333}^1 - k_{33}^0 N_{333}^2) \\
S_{12} &= \frac{1}{4\pi} (C_{12}^0 N_{1111}^1 + C_{22}^0 N_{1212}^1 + C_{32}^0 N_{1313}^1 + e_{32}^0 N_{113}^2) & S_{41} &= \frac{1}{8\pi} e_{31}^0 N_{322}^2 \\
S_{13} &= \frac{1}{4\pi} (C_{13}^0 N_{1111}^1 + C_{23}^0 N_{1212}^1 + C_{33}^0 N_{1313}^1 + e_{33}^0 N_{113}^2) & S_{42} &= \frac{1}{8\pi} e_{32}^0 N_{322}^2 \\
S_{14} &= \frac{1}{4\pi} e_{24}^0 N_{113}^2 & S_{43} &= \frac{1}{8\pi} e_{33}^0 N_{322}^2 \\
S_{15} &= \frac{1}{4\pi} e_{15}^0 N_{113}^2 & S_{44} &= \frac{1}{4\pi} [C_{44}^0 (N_{3232}^1 + N_{3322}^1 + N_{2332}^1 + N_{2233}^1) \\
& & & + e_{24}^0 (N_{232}^2 + N_{322}^2)] \\
S_{19} &= -\frac{1}{4\pi} (e_{31}^0 N_{1111}^1 + e_{32}^0 N_{1212}^1 + e_{33}^0 N_{1313}^1 - k_{33}^0 N_{113}^2) & S_{45} &= \frac{1}{4\pi} e_{15}^0 N_{322}^2 \\
S_{21} &= \frac{1}{4\pi} (C_{11}^0 N_{2121}^1 + C_{21}^0 N_{2222}^1 + C_{31}^0 N_{2323}^1 + e_{31}^0 N_{223}^2) & S_{48} &= -\frac{1}{8\pi} [e_{24}^0 (N_{3232}^1 + N_{3322}^1 + N_{2332}^1 + N_{2233}^1) \\
& & & - k_{22}^0 (N_{232}^2 + N_{322}^2)] \\
S_{22} &= \frac{1}{4\pi} (C_{12}^0 N_{2121}^1 + C_{21}^0 N_{2222}^1 + C_{32}^0 N_{2323}^1 + e_{32}^0 N_{223}^2) & S_{51} &= \frac{1}{8\pi} e_{31}^0 N_{311}^2 \\
S_{23} &= \frac{1}{4\pi} (C_{13}^0 N_{2121}^1 + C_{23}^0 N_{2222}^1 + C_{33}^0 N_{2323}^1 + e_{33}^0 N_{223}^2) & S_{52} &= \frac{1}{8\pi} e_{32}^0 N_{311}^2 \\
S_{24} &= \frac{1}{4\pi} e_{24}^0 N_{223}^2 & S_{53} &= \frac{1}{8\pi} e_{33}^0 N_{311}^2 \\
S_{25} &= \frac{1}{4\pi} e_{15}^0 N_{223}^2 & S_{54} &= \frac{1}{4\pi} e_{24}^0 N_{311}^2 \\
S_{29} &= -\frac{1}{4\pi} (e_{31}^0 N_{2121}^1 + e_{32}^0 N_{2222}^1 + e_{33}^0 N_{2323}^1 - k_{33}^0 N_{223}^2) & S_{55} &= \frac{1}{4\pi} [C_{55}^0 (N_{1133}^1 + N_{1313}^1 + N_{3113}^1 + N_{3311}^1) \\
& & & + e_{15}^0 (N_{311}^2 + N_{131}^2)] \\
S_{31} &= \frac{1}{4\pi} (C_{11}^0 N_{3131}^1 + C_{21}^0 N_{3232}^1 + C_{31}^0 N_{3333}^1 + e_{31}^0 N_{333}^2) & S_{57} &= -\frac{1}{8\pi} [e_{15}^0 (N_{1133}^1 + N_{1313}^1 + N_{3113}^1 + N_{3311}^1) \\
& & & - k_{11}^0 (N_{311}^2 + N_{131}^2)] \\
S_{32} &= \frac{1}{4\pi} (C_{12}^0 N_{3131}^1 + C_{22}^0 N_{3232}^1 + C_{32}^0 N_{3333}^1 + e_{32}^0 N_{333}^2) & S_{66} &= \frac{1}{4\pi} C_{66}^0 (N_{1122}^1 + N_{1221}^1 + N_{2112}^1 + N_{2211}^1) \\
S_{33} &= \frac{1}{4\pi} (C_{13}^0 N_{3131}^1 + C_{23}^0 N_{3232}^1 + C_{33}^0 N_{3333}^1 + e_{33}^0 N_{333}^2) & S_{75} &= -\frac{1}{2\pi} [C_{13}^0 (N_{311}^2 + N_{131}^2) + e_{15}^0 N_{11}^3] \\
S_{34} &= \frac{1}{4\pi} e_{24}^0 N_{333}^2 \\
S_{35} &= \frac{1}{4\pi} e_{15}^0 N_{333}^2
\end{aligned}$$

$$S_{77} = \frac{1}{4\pi} [e_{15}^0 (N_{311}^2 + N_{131}^2) - k_{11}^0 N_{11}^3]$$

$$S_{84} = -\frac{1}{2\pi} [C_{44}^0 (N_{322}^2 + N_{232}^2) + e_{24}^0 N_{22}^3]$$

$$S_{88} = \frac{1}{4\pi} [e_{24}^0 (N_{322}^2 + N_{232}^2) - k_{22}^0 N_{22}^3]$$

$$S_{91} = -\frac{1}{4\pi} (C_{11}^0 N_{113}^2 + C_{12}^0 N_{223}^2 + C_{31}^0 N_{333}^2 + e_{31}^0 N_{33}^3)$$

$$S_{92} = -\frac{1}{4\pi} (C_{12}^0 N_{113}^2 + C_{22}^0 N_{223}^2 + C_{32}^0 N_{333}^2 + e_{32}^0 N_{33}^3)$$

$$S_{93} = -\frac{1}{4\pi} (C_{13}^0 N_{113}^2 + C_{23}^0 N_{223}^2 + C_{33}^0 N_{333}^2 + e_{33}^0 N_{33}^3)$$

$$S_{99} = \frac{1}{4\pi} (e_{31}^0 N_{113}^2 + e_{32}^0 N_{223}^2 + e_{33}^0 N_{333}^2 - k_{33}^0 N_{33}^3)$$

where the results of N^1 , N^2 and N^3 have been shown in Wang (1992a,b).

References

- Ansgar, B.S. et al., 1996. Ferroelastic properties of lead Zirconate Titanate Ceramics. *J. Am. Ceram. Soc.* 79 (10), 2637–2640.
- Barnett, D.M., Lothe, J., 1975. Dislocations and line charges in anisotropic piezoelectric insulators. *Phys. Status. Solidi B* (67), 105–117.
- Benveniste, Y., 1992. The determination of the elastic and electric fields in a piezoelectric inhomogeneity. *J. Appl. Phys.* 72 (3), 1086–1095.
- Benveniste, Y., Dvorak, G.J., 1992. Uniform fields and universal relations in piezoelectric composites. *J. Mech. Phys. Solids* 40 (6), 1295–1312.
- Cao, H., Evans, A.G., 1993. Nonlinear deformation of ferroelectric ceramics. *J. Am. Ceram. Soc.* 76 (4), 890–896.
- Chen, Xi, Fang, DaiNing, Hwang, Keh-Chih, 1997a. A mesoscopic model of the constitutive behavior of monocrystalline ferroelectrics. *Smart Mat. Struct.* 6, 145–151.
- Chen, Xi, Fang, DaiNing, Hwang, Keh-Chih, 1997b. Micromechanics simulation of ferroelectric polarization switching. *Acta Mater.* 45 (8), 3181–3189.
- Chuang, H.T., Kim, H.G., 1987. Characteristics of domain in tetragonal phase PZT ceramics. *Ferroelectrics* 76, 327–333.
- Deeg, W.F., 1980. The analysis of dislocation, cracks, and inclusion problem in piezoelectric solids. Ph.D. dissertation. Stanford University.
- Dunn, M.L., 1995. Effects of grain shape anisotropy, porosity, and microcracks on the elastic and dielectric constants of polycrystalline piezoelectric ceramics. *J. Appl. Phys.* 78 (3), 1533–1541.
- Dunn, M.L., Taya, M., 1993a. Micromechanics predictions of the effective electroelastic modulus of piezoelectric composites. *Int. J. Solids Struct.* 30 (2), 161–175.
- Dunn, M.L., Taya, M., 1993b. Electromechanical properties of porous piezoelectric ceramics. *J. Am. Ceram. Soc.* 76 (7), 1697–1706.
- Dunn, M.L., Taya, M., 1993c. An analysis of piezoelectric composite materials containing ellipsoidal inhomogeneities. *Proc. R. Soc. Lond. A* 443, 265–287.
- Hwang, S.C., Lynch, C.S., McMeeking, R.M., 1995. Ferroelectric/ferroelastic interactions and a polarization switching model. *Acta Metall. Mater.* 43 (5), 2073–2084.
- Jaff, B., Cook, W.R., Jaff, H., 1971. Piezoelectric ceramic. Academic press, New York.
- Kahn, M., 1985. Acoustic and elastic properties of Pzceramics with anisotropic pores. *J. Am. Ceram. Soc.* 68, 623–628.
- Kuo, W.S., Huang, J.H., 1997. On the effective electroelastic properties of piezoelectric composites containing spatially oriented inclusions. *Int. J. Solids Struct.* 34 (19), 2445–2461.
- Lynch, C.S. et al., 1995. Electric field induced cracking in ferroelectric ceramics. *Ferroelectrics* 166, 11–30.
- Marutak, M., 1965. A calculation of physical constants of lead zirconate barium titanate. *J. Phys. Soc. Jpn.* 11 (8), 807–814.
- Merz, W.J., 1956. Switching time in ferroelectric BaTiO₃ and its dependence on crystal thickness. *J. Appl. Phys.* 27 (8), 938–943.
- Nan, C.-W., Clarke, D.R., 1996. Piezoelectric modulus of piezoelectric ceramics. *J. Am. Ceram. Soc.* 79 (10), 2536–2566.
- Wang, B., 1992a. Three-dimensional analysis of an ellipsoidal inclusion in a piezoelectric material. *Int. J. Solids Struct.* 29 (3), 293–308.
- Wang, B., 1992b. Three-dimensional analysis of a flat elliptical crack in a piezoelectric material. *Int. J. Engng. Sci.* 30 (6), 781–791.
- Wang, B., 1994. Effective behavior of piezoelectric composites. *Appl. Mech. Rev.* 47 (1), s112–s121.
- Xu, Y., 1991. Ferroelectric materials and their applications. North-Holland, New York.
- Zenon, B., 1994. Optical microscopic mapping of the domain structure of BaTiO₃ microcrystals. *Ferroelectrics* 157, 13–18.
- Zhang, Q.M. et al., 1997. Change of the weak-field properties of Pb(ZrTi)O₃ piezoceramics with the compressive uniaxial stresses and its links to the effect of dopants on the stability of the polarizations in the materials. *J. Mater. Res.* 12 (1), 226–234.